

Disordered Phases **Hot Paper**International Edition: DOI: 10.1002/anie.202001922
German Edition: DOI: 10.1002/ange.202001922

A Pressure-Induced Inverse Order–Disorder Transition in Double Perovskites

Zheng Deng,* Chang-Jong Kang,* Mark Croft, Wenmin Li, Xi Shen, Jianfa Zhao, Richeng Yu, Changqing Jin,* Gabriel Kotliar, Sizhan Liu, Trevor A. Tyson, Ryan Tappero, and Martha Greenblatt*

Abstract: Given the consensus that pressure improves cation ordering in most of known materials, a discovery of pressure-induced disordering could require recognition of an order–disorder transition in solid-state physics/chemistry and geophysics. Double perovskites Y_2CoIrO_6 and Y_2CoRuO_6 polymorphs synthesized at 0, 6, and 15 GPa show *B*-site ordering, partial ordering, and disordering, respectively, accompanied by lattice compression and crystal structure alteration from monoclinic to orthorhombic symmetry. Correspondingly, the long-range ferrimagnetic ordering in the *B*-site ordered samples are gradually overwhelmed by *B*-site disorder. Theoretical calculations suggest that unusual unit-cell compressions under external pressures unexpectedly stabilize the disordered phases of Y_2CoIrO_6 and Y_2CoRuO_6 .

Introduction

As a fundamental thermodynamic variable, pressure is experimentally controllable to tunes and alters structural, chemical, physical, and mechanical properties. It can also extend new phases by altering crystal structures or atomic orders of an existing material. The discovery of post-perovskite phases under extremely high-pressure successfully explained the origin of the *D'* seismic discontinuity in lower mantle.^[1,2] By modifying long-range hydrogen ordering, pressure can modify the ferroelectric state of the potassium dihydrogen phosphates.^[3,4]

Order–disorder effects in materials are of fundamental interest to solid state sciences.^[5–7] Polymorphs with identical chemical formula, but different ordering degrees, can have altered crystal symmetries and hence distinct properties. Order–disorder transitions have been experimentally and theoretically studied in alloys and mineralogical systems.^[6–12] Pressure has also been applied to modify atomic ordering, owing to the development of high-pressure techniques.^[5,13–16] Obtaining insight of pressure-controlled order–disorder transition could generate new techniques to improve performances of materials, and build more rational models of transport properties of minerals that constitute the mantle and deeper interiors of our planet, as the post-perovskite demonstrated. Double perovskites (DP) with formula $A_2B'B''O_6$ containing exactly 50% *B'* and 50% *B''* cations at the *B*-site, can form *B*-site ordered, partially ordered or disordered polymorphs.^[17,18] Hence this family provides ideal models to investigate order–disorder effects, which have attracted the extensive attention of researchers.^[19–23]

Generally large differences in oxidation states and cation radii of *B'* and *B''* tend to enhance cation order. In this case the disordering will raise the energy of a DP, owing to local strain/distortion from neighboring *B'-B''/B''-B''* and electrostatic repulsion from highly charged *B''-B''* (*B''* is defined with higher oxidation state than *B'*), thereby stabilizing the *B*-site ordered phase.^[22] The disordered phases will also have larger lattice volumes, since the distance of neighboring *B''-B''* will be additionally enlarged owing to strong repulsion.^[20] The application of pressure always drives smaller cell volumes and consequently, stabilizes the cation ordered phase over the disordered phase. In multiple experiments, synthesis pressure has been used to improve *B*-site order of the ambient-phases.^[24–26] For example, Sr_2FeReO_6 obtained under ambient pressure has $s \approx 0.7$ ($s \equiv 2\omega_B - 1$, with ω_B for occupancy of *B'*

[*] Dr. Z. Deng, Dr. W. Li, Dr. X. Shen, Dr. J. Zhao, Prof. Dr. R. Yu, Prof. Dr. C. Jin
Institute of Physics, Chinese Academy of Sciences;
School of Physics, University of Chinese Academy of Sciences
Beijing, 100190 (China)
E-mail: dengzheng@iphy.ac.cn
jin@iphy.ac.cn

Dr. Z. Deng, Prof. Dr. M. Greenblatt
Department of Chemistry and Chemical Biology
Rutgers, the State University of New Jersey
610 Taylor Road, Piscataway, NJ 08854 (USA)
E-mail: greenbla@chem.rutgers.edu

Dr. C.-J. Kang, Prof. Dr. M. Croft, Prof. Dr. G. Kotliar
Department of Physics and Astronomy
Rutgers, the State University of New Jersey
136 Frelinghuysen Road, Piscataway, NJ 08854 (USA)
E-mail: ck620@physics.rutgers.edu

Dr. S. Liu, Prof. Dr. T. A. Tyson
Department of Physics, New Jersey Institute of Technology
Newark, NJ 07102 (USA)

Dr. R. Tappero
Photon Sciences Division, Brookhaven National Laboratory
Upton, NY 11973 (USA)

Supporting information (experimental details, chemical composition analyses by EDX, crystal-structure parameters, valance states studied by XANES, electron-diffraction analyses, specific heat data, and physical picture of unit cell volume change during order–disorder transition in double perovskites) and the ORCID identification number(s) for the author(s) of this article can be found under: <https://doi.org/10.1002/anie.202001922>.

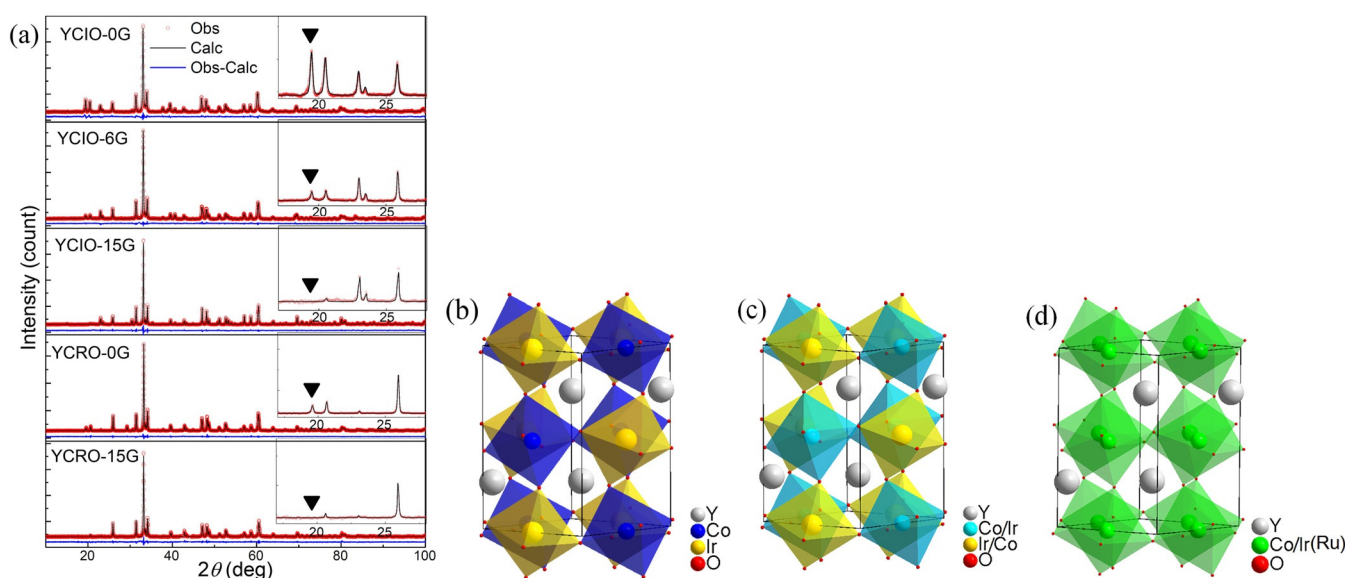


Figure 1. Rietveld refinements and representations of all of the phases. a) Room-temperature Rietveld refined PXD profiles of YCIO-0G, YCIO-6G, YCIO-15G, YCRO-0G, and YCRO-15G are plotted from top to bottom. Insets show peaks around 19.5°, and black triangles mark the positions of (011) peaks. The crystal structures of b) YCIO-0G, c) YCIO-6G, and d) YCIO-15G and YCRO-15G show *B*-site order, partial order, and disorder, respectively.

cation at the expected site) while the high-pressure-synthesized sample is nearly completely ordered ($s \approx 1$).^[27]

This simple mechanism for pressure-induced ordering in DPs works well until one finds higher synthesis pressure decreasing *B*-site order in Y_2CoIrO_6 (YCIO) and Y_2CoRuO_6 (YCRO) as shown in this work. The former is a new DP while the ordered phase of the latter was recently reported.^[28] In YCIO the ordering degree decreases from $s = 0.854$ for ambient pressure synthesized sample (YCIO-0G) to $s = 0.454$ for sample synthesized at 6 GPa (YCIO-6G), and finally to $s = 0$ for sample synthesized at 15 GPa (YCIO-15G). For YCRO s changes from 0.84 of ambient pressure sample (YCRO-0G) to 0 of 15 GPa one (YCRO-15G). Correspondingly, substantial decreases of unit cell volume of YCIO and YCRO are experimentally observed. For both compounds, the structure symmetries and magnetic properties also synchronously change with the loss of *B*-site ordering.

Results and Discussion

The high scattering contrast to X-ray between Co and Ir/Ru allows us to quantitatively analyze the *B*-site ordering degrees. The YCIO-0G and YCRO-0G samples show nearly complete rock-salt ordered *B'*- and *B''*-sublattices, while YCIO-6G shows *B*-site partial order, whereas YCIO-15G and YCRO-15G show complete *B*-site disorder. Figure 1a displays room-temperature powder X-ray diffractions (PXD) patterns for YCIO-0G,

YCIO-6G, and YCIO-15G. The top part shows PXD pattern for a typical *B*-site rock-salt ordered DP with monoclinic $P2_1/n$ symmetry. In this model, *B'*(Co)-site and *B''*(Ir)-site cations occupy two separate crystallographic sites, $2c$ ($1/2, 0, 1/2$) and $2d$ ($1/2, 0, 0$), respectively. The main difference among the top three figure parts is the intensity of the peaks around 19.5°, which are from the ordered *B*-site reflections ((011) peaks).^[29] In the insets of Figure 1a the normalized (011) peak is pronounced for YCIO-0G, while it decays dramatically for YCIO-6G and vanishes for YCIO-15G, indicating the loss of *B*-site order. Consequently, YCIO-0G and YCIO-6G are refined with $P2_1/n$ space group by Rietveld analysis. The obtained parameters are tabulated in Table 1 and the Supporting Information, Table S5. Figure 1b demonstrates that YCIO-0G is an isostructural analogue of $\text{La}_2\text{CoIrO}_6$, but with stronger CoO_6 - IrO_6 octahedral tilting.^[30] For YCIO-0G, the bond valence sum (BVS) is 2.12 for Co and 4.09 for Ir, consistent with Co^{2+} and Ir^{4+} evidenced by X-ray absorption

Table 1: Selected structural parameters as determined by Rietveld refinements.

Parameters	YCIO-0G	YCIO-6G	YCIO-15G	YCRO-0G	YCRO-15G
P_{synth} [GPa] ^[a]	0	6	15	0	15
Space group	$P2_1/n$	$P2_1/n$	$Pbnm$	$P2_1/n$	$Pbnm$
a [Å]	5.2690(1)	5.2585(1)	5.2515(1)	5.2683(1)	5.2448(1)
b [Å]	5.6910(1)	5.6902(1)	5.6856(1)	5.7073(1)	5.6878(2)
c [Å]	7.5720(1)	7.5621(2)	7.5589(1)	7.5561(1)	7.5461(2)
β [°]	90.099(2)	89.997(4)	90	89.942(2)	90
V [Å ³]	227.053(7)	226.268(12)	225.696(4)	227.198(6)	225.112(14)
R_{wp} [%], R_{p} [%]	2.06, 1.52	2.62, 2.04	2.38, 1.71	2.54, 1.86	2.18, 1.69
<i>B'</i> - <i>B''</i> antisite [%], s	7.3, 0.854	27.3, 0.454	50, 0	8.0, 0.840	50, 0
BVS- <i>B'</i>	$\text{Co}^{2.12+}$	N/A	N/A	$\text{Co}^{2.05+}$	N/A
BVS- <i>B''</i>	$\text{Ir}^{4.09+}$	N/A	N/A	$\text{Ru}^{3.98+}$	N/A

[a] Synthesis pressure.

near-edge spectroscopy (XANES) results (Supporting Information, Figures S5, S6).

The major difference between YCIO-0G and YCIO-6G is the decreasing *B*-site order (Figure 1c) and smaller cell volume with higher pressure ($s_{\text{YCIO-0G}} = 0.854$, $s_{\text{YCIO-6G}} = 0.454$; $V_{\text{YCIO-0G}} = 227.053 \text{ \AA}^3$, $V_{\text{YCIO-6G}} = 226.268 \text{ \AA}^3$). The cell volume of YCIO-15G decreases to 225.696 \AA^3 . Initial $P2_1/n$ refinement of YCIO-15G yielded $s = 0.038$,^[31] a value extremely close to complete *B*-site disorder. Therefore, orthorhombic symmetry with space group *Pbnm* for *B*-site disordered DP was used.^[22] In this model, the $2c$ and $2d$ sites in $P2_1/n$ merge into one crystallographic site, $4a$ (0, 0.5, 0), which exactly contain 50% Co and 50% Ir for the case of YCIO (Figure 1d). Thus YCIO-15G possesses the lowest *B*-site order ($s = 0$) and smallest lattice volume. The space groups of *B*-site ordered YCIO-0G and disordered YCIO-15G are further confirmed by a high resolution transmission electron microscopy: along the [100] zone-axis the $(0\ 2k+1\ l)$ -serial spots in the selected area electron diffraction patterns are present for YCIO-0G, but extinct for YCIO-15G (Supporting Information, Figure S7). In short, we obtained three phases of YCIO with three degrees of *B*-site ordering: a nearly completely ordered YCIO-0G, a partially ordered YCIO-6G and a completely disordered YCIO-15G. It is noteworthy that XANES measurements suggest a slight valence change of Co^{2+} and Ir^{4+} in YCIO-0G to $\text{Co}^{2.14+}$ and $\text{Ir}^{3.70+}$ in YCIO-15G (Supporting Information, Figures S5, S6).

Similar pressure-induced order–disorder transition occurs in YCRO. YCRO-0G is isostructural to YCIO-0G with $s_{\text{YCRO-0G}} = 0.84$, consistent with previous report.^[28] In contrast, in the inset of Figure 1a the extinct (011) peak on the PXD pattern

of YCRO-15G implies complete *B*-site disorder. Rietveld refinement indicates that YCRO-15G is isostructural to YCIO-15G (Table 1 and Figure 1d). The lattice volume $V = 225.112 \text{ \AA}^3$ is substantially smaller than that of YCRO-0G ($V = 227.198 \text{ \AA}^3$).^[28]

The degrees of *B*-site order significantly influence the magnetic behaviors of both YCIO and YCRO. Similar to previous studies magnetic frustration, which is induced by the *B'*–*B''* antisite,^[24,27,32] weakens long-range magnetic ordering in *B*-site ordered DPs. Temperature-dependent magnetization ($M(T)$) in Figure 2a shows that a ferromagnetic (FM)-like phase transition occurs in YCIO-0G upon cooling down. The derivative of susceptibility was used to determine the transition temperature (T_C) as 123 K. The divergence between zero field cooling (ZFC) and field cooling (FC) and the λ -shape feature indicate the presence of magnetic frustration, which is presumably due to minor *B*-site disorder. Nevertheless, the long-range magnetic ordering phase transition is evidenced by a clear λ -shape peak in the specific heat versus temperature ($C_p(T)$) curve (Supporting Information, Figure S8). The saturated hysteresis loop ($M(H)$) in Figure 2d evidences a robust magnetic order. Above T_C , a hyperbolic-like inverse susceptibility ($\chi^{-1}(T)$) is a feature of ferrimagnetism (FiM).^[28] The Curie–Weiss law, $1/\chi = (T - \theta)/C$, is used for fitting the data in the high-temperature region (250–400 K), which yields a Curie constant $C = 2.84 \text{ emu K mol}^{-1} \text{ Oe}^{-1}$ with an effective moment $\mu_{\text{eff}} = 4.77 \mu_B/\text{f.u.}$ (f.u. = formula unit) and the paramagnetic temperature θ (sum of magnetic exchange interactions) = -18.6 K . Both μ_{eff} and θ are comparable to those of $\text{La}_2\text{CoIrO}_6$.^[30]

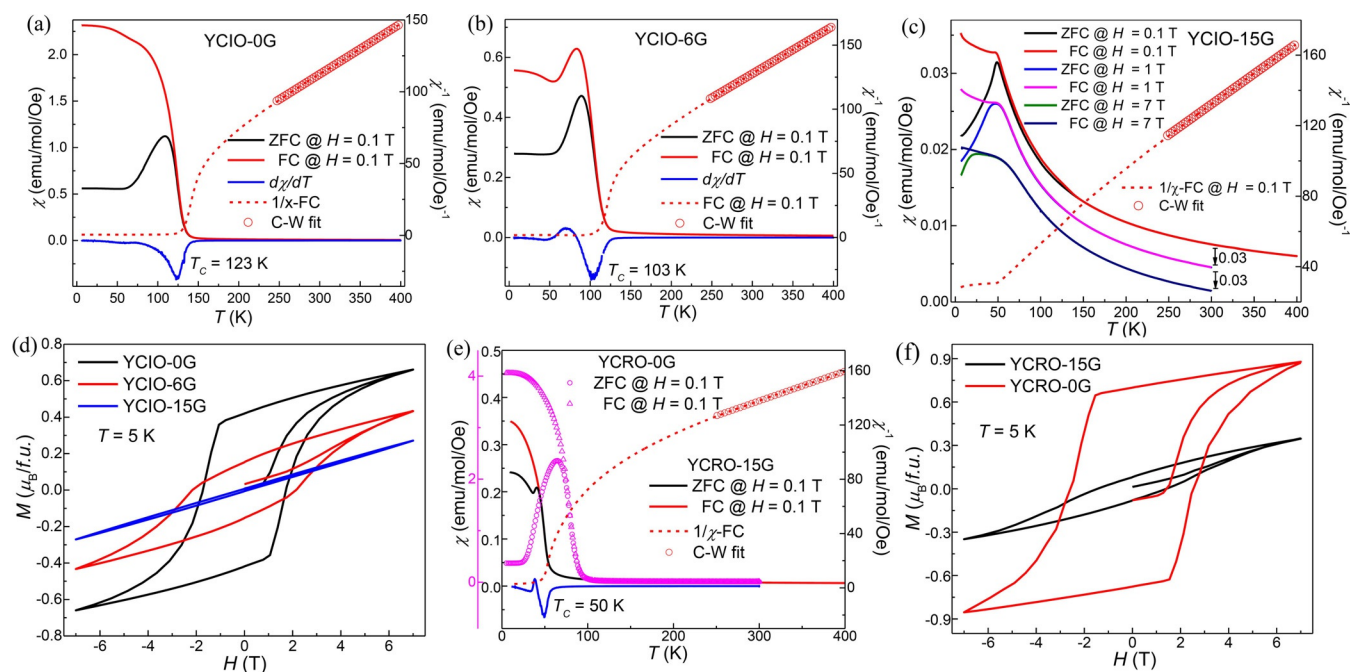


Figure 2. Magnetic properties of Y_2CoIrO_6 synthesized under various pressures. a), b) Temperature dependence of magnetization and inverse susceptibility at $H = 0.1 \text{ T}$ for a) YCIO-0G and b) YCIO-6G. c) $M(T)$ at varying fields and $\chi^{-1}(T)$ at $H = 0.1 \text{ T}$ for YCIO-15G. d) Field dependence of magnetization measured at 5 K for YCIO-0G, YCIO-6G, and YCIO-15G. e) $M(T)$ and $\chi^{-1}(T)$ at $H = 0.1 \text{ T}$ for YCRO-0G and YCRO-15G. Purple γ -axis: YCRO-0G, black axis: YCRO-15G. f) $M(H)$ measured at 5 K for YCRO-0G and YCRO-15G.

In Figure 2b, YCIO-6G also shows FiM-like transitions at 103 K, a lower temperature than T_C of YCIO-0G. However, the weakened magnetization of YCIO-6G than that of YCIO-0G in either $M(T)$ or $M(H)$ (Figure 2d), along with the broader hump around T_C of $C_p(T)$ (Supporting Information, Figure S8) indicate stronger magnetic frustration and loss of magnetic ordering. We obtain $\mu_{\text{eff}} = 4.72 \mu_B/\text{f.u.}$ and $\theta = -41.3$ K from the Curie–Weiss fit. In Figure 2c, the magnetic behaviors of YCIO-15G are relatively complex. Under $H = 0.1$ T, the shape peak at 50 K suggests an antiferromagnetic (AFM) transition. However, with the increasing H , the peak is being smeared and the divergence between ZFC and FC is vanishing. In Figure 2d the $M(H)$ loop for YCIO-15G is slightly open even at $H \approx 6$ T. $C_p(T)$ of YCIO-15G shows no visible sign of phase transition (Supporting Information, Figure S8). These features demonstrate a spin-glass-like short-range magnetic order, which is due to completely disordered $B'B''$ -site cations. We obtain $\mu_{\text{eff}} = 4.80 \mu_B/\text{f.u.}$ and $\theta = -82.6$ K. The marginal change of effective moments (4.72 – $4.80 \mu_B/\text{f.u.}$) among the three phases is coincident with almost unchanged d-electron configurations on Co and Ir.

A crossover from FiM to spin-glass like magnetic behavior with increasing magnetic frustration, despite of uncertain magnetic structures, has been found from YCIO-0G to YCIO-15G. Three major mechanisms can induce similar changes in $A_2B'B''O_6$: 1) variations of magnetic moments on B'/B'' site cations owing to alterations of valences;^[33] 2) distortions of $B'-O-B''$ angles;^[28,34] 3) modifications of B -site ordering degrees.^[24,32,35] In the case of YCIO, neither Co–O–Ir angles nor oxidation states of Co/Ir show more than negligible changes among the three phases. Thus the increased B -site disorder is the only factor to induce such strong magnetic fluctuation. Furthermore, significant increase of θ from -18.6 to -82.6 K, which is also evidence for increasing AFM exchange interactions, should be primarily from super-exchanges of anti-parallel nearest-neighbor Co–Co and Ir–Ir yielded by the Co–Ir antisite.

Similarly, the magnetic behaviors of YCRO also change correspondingly with different B -site ordering. As shown in Figure 2e,f, YCRO-0G exhibits a FiM transition at around 80 K with long-range magnetic ordering.^[28] YCRO-15G shows a FM-like transition at 50 K with much stronger magnetic frustration, as evidenced by an almost closed and unsaturated $M(H)$ loop in Figure 2e,f. For YCRO-15G, we obtained $\mu_{\text{eff}} = 6.03 \mu_B/\text{f.u.}$ and $\theta = -328.7$ K. The former is comparable to that of YCRO-0G ($\mu_{\text{eff}} = 5.68 \mu_B/\text{f.u.}$) while that of the latter is over 200% of the ordered phase ($\theta = -162$ K).^[28] Thus the considerable changes in magnetic behaviors between ambient and high pressure synthesized YCIO and YCRO, respectively also strongly support evidence of B -site disordering with increasing pressure.

It is essential to explain the pressure-induced order-disorder phase in this compound. As already noted, usually, pressure tends to increase cation order in a crystal structure. However, YCIO and YCRO show the opposite trend. To explain the unusual behaviors, we applied the recently proposed order-disorder theory to our compounds.^[21,36] The thermodynamic potential, $G \equiv E - TS + PV$, where E , S , and P are internal energy, entropy, and applied pressure, respec-

tively. Then at certain temperature and pressure the difference between ordered and disordered phases is according to Equation (1):

$$\Delta G \equiv G_{\text{dis}} - G_{\text{ord}} = (E_{\text{dis}} - TS_{\text{dis}} + PV_{\text{dis}}) - (E_{\text{ord}} - TS_{\text{ord}} + PV_{\text{ord}}) \\ = \Delta E - T\Delta S + P\Delta V \quad (1)$$

If $\Delta G > 0$, then the ordered phase is favorable, otherwise the disordered phase is more stable than the ordered one. Generally, with increasing disordering the internal energy tends to increase due to local strain/distortion, resulting in the first term $\Delta E > 0$. For the case of DPs, the change of internal energy is predominantly determined by the unstrained equilibrium bond lengths of $A-O$, $B'-O$, and $B''-O$ (related to cation radii) as well as their stiffness (related to valence states/strengths of the $B-O$ bond). This conclusion is consistent with the consensus that larger valence difference (Δn_B) and cation radius divergence (ΔR_B) can stabilize the ordered phase.^[36] Entropy has positive correlation with disordering degree, thus we always have $-T\Delta S < 0$. The third term, $P\Delta V$, now becomes crucial for order-disorder transition: it could promote or impede the formation of an ordered phase depending on the sign of ΔV . Furthermore, the impact of ΔV is amplified by applied pressure.

A rough approximation is that the higher-charged cation (B'') determines the average bond length of the disordered phase owing to its stronger (than that of the B') bond stiffness (see the Supporting Information, Sections 6, 7). We further propose a stricter calculation according to the statistical model proposed by Sakhnenko and Ter-Oganessian.^[21,36] Here G can be expressed as parameters s and a , where a is the reduced cubic cell lattice parameter corresponding to one $AB'_{1/2}B''_{1/2}O_3$ formula unit cell. From $\frac{\partial G}{\partial a} = 0$, the equilibrium value of a can be determined for a given values of the order parameter s and pressure P . For $A_2^{3+}B'^{2+}B''^{4+}O_6$ at ambient pressure, the equilibrium lattice constant a can be written as given in Equation (2):

$$a(s) = \frac{18\sqrt{2}l_A + (14 + 2s^2)l_{B'} + (20 - 4s^2)l_{B''}}{35 - s^2} \quad (2)$$

where l_A , $l_{B'}$, and $l_{B''}$ are unstrained equilibrium bond lengths of $A-O$, $B'-O$, and $B''-O$, respectively. The corresponding values are related to the effective cation radii. Then the equilibrium values a for disordered and ordered phases from Eq. (2) are as given in Equation (3):

$$a(s=0) = \frac{18\sqrt{2}l_A + 14l_{B'} + 20l_{B''}}{35}, \text{ and } a(s=1) = \frac{9\sqrt{2}l_A + 8l_{B'} + 8l_{B''}}{17} \quad (2)$$

When $a(s=0) > a(s=1)$, namely, $l_{B''} > \frac{7}{10}l_{B'} + \frac{3\sqrt{2}}{20}l_A$, pressure promotes B -site ordering, otherwise pressure hinders the B -site ordering.

Based on the above mechanism, we plot the general phase diagram for $A_2^{3+}B'^{2+}B''^{4+}O_6$ in Figure 3. The red line determined by the effective cation radius of Y^{3+} , that is, $l_{B''} = \frac{7}{10}l_{B'} + \frac{3\sqrt{2}}{20}l_Y$, divides the diagram into two regions: the

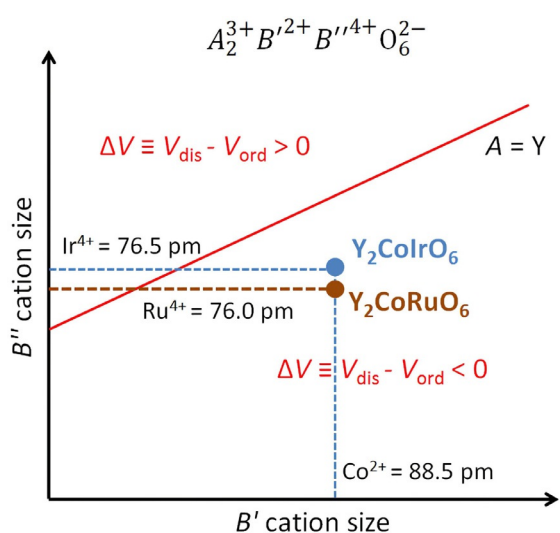


Figure 3. Diagram for $A_2^{3+}B^{2+}B''^{4+}O_6^{2-}$. There are two regions: $\Delta V > 0$ and $\Delta V < 0$, which indicate that ordered and disordered phases are preferred upon pressure, respectively. The red line is a boundary of the two regions when $A=Y$.

top region shows $V_{\text{dis}} > V_{\text{ord}}$, corresponding to pressure-induced ordering, while the bottom area is just the opposite. Since the size of cation Co^{2+} (88.5 pm) is substantially larger than that of Ir^{4+} (76.5 pm) and Ru^{4+} (76.0 pm), YCIO and YCRO are located at bottom side.

Additionally, in Equation (1), when P is set, the order-disorder transition temperature ($T_{\text{o-d}}$) is therefore obtained from the relation $\Delta G=0$. With the oxidation states determined by XANES, which are Co^{2+} and Ir^{4+} for YCIO-0G, $\text{Co}^{2.14+}$ and $\text{Ir}^{3.7+}$ for YCIO-15G, our calculations show $T_{\text{o-d}}=2386$ K at $P=0$ GPa and $T_{\text{o-d}}=1172$ K at $P=15$ GPa. We assume the oxidation states of YCRO-15G maintain Co^{2+} and Ru^{4+} in YCRO-0G,^[28] owing to lack of corresponding XANES data. Then $T_{\text{o-d}}=1389$ K at $P=0$ GPa and $T_{\text{o-d}}=619$ K at $P=15$ GPa are obtained for YCRO. Regardless of

the relative quantities, the decreasing tendency of $T_{\text{o-d}}$ upon pressure further supports the finding that pressure induces B -site disorder in YCIO and YCRO. It is noteworthy that if the configuration of Co^{2+} and Ir^{4+} is used at $P=15$ GPa, the calculated $T_{\text{o-d}}=1337$ K. This indicates that the slight charge transfer between Co and Ir indeed benefits pressure-induced order-disorder transition in YCIO.

High pressure has been widely used to synthesize B -site ordered or disordered DPs for decades. However, surprisingly, YCIO and YCRO are the first two DPs, to the best of our knowledge, to show pressure-induced disorder. Typically, increasing pressure is used to improve cation order rather than disorder, based on the aforementioned assumption that decreasing cell volume leads to higher ordering.^[5] Furthermore, B -site ordered $A_2B^{m+}B''^{n+}O_6$ compounds with $n > 5$, are overwhelmingly more numerous than others. Generally it is difficult to induce disorder by overcoming the electrostatic repulsions between the highly charged B'' -cations.^[22] The only group of DPs with small n and minimum Δn_B ($\Delta n_B = n - m$) is $A_2B^{2+}B''^{4+}O_6$. Additionally, the slight charge transfer from Co to Ir with increasing P , further decreases the valence and bond length difference between B' and B'' -site cations. As a result, $T_{\text{o-d}}$ is further reduced under pressure. Owing to the above features, pressure-induced disordering is observed in YCIO and YCRO. It is noteworthy that both ambient-pressure-synthesized B -site ordered YCIO and YCRO can be directly converted into B -site disordered phases under 15 PGa within a half-hour. Thus the rapid order-disorder transformations rule out a mechanism controlled by kinetic effects. Nevertheless, we do not exclude a scenario that the disordered phase happens in the regime where a phase transition should have occurred, and the disordered structure that is observed is metastable, but the transition to the new stable ordered state might be realized at a higher pressure.

We now turn to investigate the electronic structure of YCIO-0G and YCRO-0G, the B -site ordered phases. The experimental crystal structure $P2_1/n$ was adopted for density functional theory (DFT) calculations.^[37–40] Figure 4 shows the

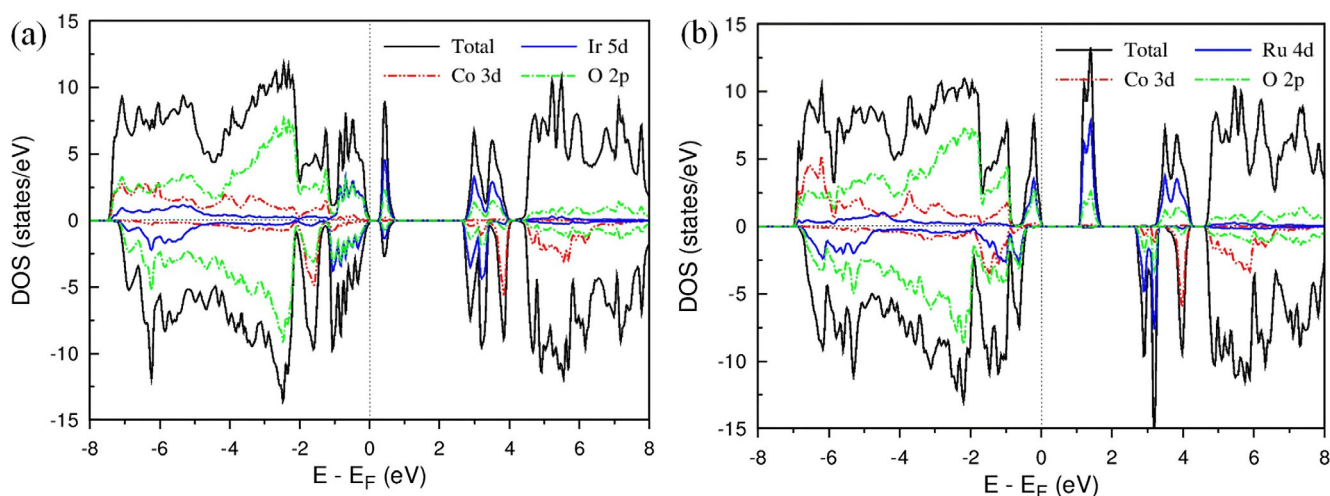


Figure 4. Total and partial density of states of a) Y_2CoIrO_6 and b) Y_2CoRuO_6 with ferrimagnetic order from GGA+SOC+U calculations. The Fermi level is set to zero in the plot. The positive and negative values in DOS correspond to spin up and down, respectively.

electronic density of states with FiM ordering, YCIO-0G and YCRO-0G are insulating with band gaps of 0.28 and 1.13 eV, respectively. The electron occupation numbers are: 6.73 and 5.30 for Co 3d and Ir 5d in YCIO-0G; 6.76 and 4.57 for Co 3d and Ru 4d in YCRO-0G, respectively. Considering the hybridization with O 2p orbital, it suggests Co^{2+} ($3d^7$) and Ir^{4+} ($5d^5$) in YCIO-0G, Co^{2+} ($3d^7$) and Ru^{4+} ($4d^4$) in YCRO-0G,^[28] consistent with the XANES experiments. In YCIO-0G, we obtain spin moments $\mu_S(\text{Co}) = 2.69 \mu_B$, $\mu_S(\text{Ir}) = -0.26 \mu_B$, orbital moments $\mu_L(\text{Co}) = 0.12 \mu_B$, $\mu_L(\text{Ir}) = -0.26 \mu_B$, and total moments $\mu_{\text{tot}}(\text{Co}) = 2.81 \mu_B$, $\mu_{\text{tot}}(\text{Ir}) = -0.64 \mu_B$, where the minus sign indicates the opposite direction to the magnetic moment of Co. Therefore, the net magnetic moment is $2.46 \mu_B/\text{f.u.}$ by taking into account the induced magnetic moment in the interstitial region. It is much larger than the saturated magnetization (μ_{sat}) of about $0.6 \mu_B/\text{f.u.}$ in Figure 2d, presumably due to canting effect. In YCRO-0G, the moments are $\mu_S(\text{Co}) = 2.70 \mu_B$, $\mu_S(\text{Ru}) = -1.35 \mu_B$, $\mu_L(\text{Co}) = 0.15 \mu_B$, $\mu_L(\text{Ru}) = -0.16 \mu_B$, and $\mu_{\text{tot}}(\text{Co}) = 2.85 \mu_B$, $\mu_{\text{tot}}(\text{Ru}) = -1.51 \mu_B$. The net magnetic moment $1.01 \mu_B/\text{f.u.}$ is also slightly larger than the experimental result of $\mu_{\text{sat}} \approx 0.8 \mu_B/\text{f.u.}$ ^[28]

Conclusion

We synthesized a new completely *B*-site ordered double perovskite, Y_2CoIrO_6 , at ambient pressure. Surprisingly, when Y_2CoIrO_6 is synthesized at high pressure, 6 and 15 GPa, the phases form with smaller unit cell volume, but contrary to expectations, with partial or complete *B*-site disordering, respectively. The *B*-site ordered (0 GPa) and partially ordered (6 GPa) phases crystallize in a monoclinic ($P2_1/n$) structure, while the disordered (15 GPa) one forms in orthorhombic ($Pbnm$) symmetry. The increasing Co-Ir anti-site disorder generates magnetic frustrations that weaken and finally break long-range ferrimagnetic ordering in the *B*-site ordered Y_2CoIrO_6 . Nearly identical phenomenon is also found in *B*-site ordered (0 GPa) and disordered (15 GPa) Y_2CoRuO_6 . Both ambient-pressure-synthesized *B*-site ordered Y_2CoIrO_6 and Y_2CoRuO_6 can be directly converted rapidly to *B*-site disordered phases under 15 GPa. With both DFT calculations and the statistical model of atomic ordering, we infer that this unique pressure-induced order-to-disorder transition in Y_2CoIrO_6 and Y_2CoRuO_6 are primarily due to the substantially larger effective cation size of Co^{2+} compared to that of Ir^{4+} (Ru^{4+}), thereby rendering $\Delta V = V_{\text{dis}} - V_{\text{ord}} < 0$. Thus $\Delta G = G_{\text{dis}} - G_{\text{ord}} = \Delta E - T\Delta S + P\Delta V < 0$ at high pressure owing to the negative term $P\Delta V$, so that this unusual volume change ($V_{\text{dis}} < V_{\text{ord}}$ at high P) stabilizes the disordered phase with increasing pressure. Pressure-induced disorder in Y_2CoIrO_6 and Y_2CoRuO_6 is contrary to traditional theories of order-disorder mechanism and will lead to reconsideration of pressure effects in solid state sciences.

Acknowledgements

The authors wish to gratefully acknowledge D. Walker, X.-H. Xu, F.-X. Jiang, X. Li, and J.-G. Cheng for helpful discussions.

C.-J.K., G.K., and M.G. were supported by the U. S. Department of Energy, Office of Science, Basic Energy Science as a part of the Computational Materials Science Program through the Center for Computational Design of Functional Strongly Correlated Materials and Theoretical Spectroscopy. M.G. also acknowledges support of NSF-DMR-1507252 grant. Regarding the experiments at the Brookhaven National Synchrotron Light Source (NSLS-II): the support under DOE BES(DE-SC0012704) and NSF Grant DMR-1809931 are acknowledged; and the authors also gratefully acknowledge the aid of S. Ehrlich and S. Khalid. Works at IOPCAS were supported by MOST (No. 2018YFA03057001 and 2017YFB0405703) & NSF (No. 11921004, 11820101003, 11534016, and 11974407) of China through research projects. Z.D. also acknowledges support of the Youth Innovation Promotion Association of CAS (No. 2020007).

Conflict of interest

The authors declare no conflict of interest.

Keywords: double perovskites · lattice compression · magnetic frustration · pressure-induced *B*-site disorder · statistical model

How to cite: *Angew. Chem. Int. Ed.* **2020**, *59*, 8240–8246
Angew. Chem. **2020**, *132*, 8317–8323

- [1] M. Murakami, K. Hirose, K. Kawamura, N. Sata, Y. Ohishi, *Science* **2004**, *304*, 855–858.
- [2] A. R. Oganov, S. Ono, *Nature* **2004**, *430*, 445.
- [3] M. Tokunaga, T. Matsubar, *Prog. Theor. Phys.* **1966**, *35*, 581.
- [4] D. A. Boysen, S. M. Haile, *Chem. Mater.* **2004**, *16*, 693.
- [5] R. M. Hazen, A. Navrotsky, *Am. Mineral.* **1996**, *81*, 1021.
- [6] R. M. Hazen, H. Yang, *Science* **1997**, *277*, 1965.
- [7] M. Yang, J. Oro-Sole, J. A. Rodgers, A. B. Jorge, A. Fuytes, J. P. Attfield, *Nat. Chem.* **2011**, *3*, 47.
- [8] S. Rocha, P. Thibaudeau, *J. Phys. Condens. Matter* **2003**, *15*, 7103.
- [9] V. M. Talanov, V. B. Shirokov, *Acta Crystallogr. Sect. A* **2014**, *70*, 49.
- [10] D. B. Miracle, O. N. Senkov, *Acta Mater.* **2017**, *122*, 448.
- [11] A. Asamitsu, Y. Moritomo, Y. Tomioka, T. Arima, Y. Tokura, *Nature* **1995**, *373*, 407.
- [12] A. Navrotsky, *Am. Mineral.* **1994**, *79*, 589–605.
- [13] G. Shen, H. K. Mao, *Rep. Prog. Phys.* **2017**, *80*, 016101.
- [14] J. H. Chen, R. Li, J. B. Parise, D. J. Weidner, *Am. Mineral.* **1996**, *81*, 1519.
- [15] Y. Lee, T. Vogt, J. A. Hriljac, J. B. Parise, G. Artioli, *J. Am. Chem. Soc.* **2002**, *124*, 5466.
- [16] M.-R. Li, D. Walker, M. Retuerto, T. Sarkar, J. Hadermann, P. Stephens, M. Croft, A. Ignatov, J. Hemberger, I. Nowik, K. Ramanujachary, P. Halasyamani, T. Thao Tran, S. Mukherjee, T. Dasgupta, M. Greenblatt, *Angew. Chem. Int. Ed.* **2013**, *52*, 8406–8410; *Angew. Chem.* **2013**, *125*, 8564–8568.
- [17] Y.-H. Huang, R. I. Dass, Z.-L. Xing, J. B. Goodenough, *Science* **2006**, *312*, 254.
- [18] Q. Li, Y. G. Wang, W. C. Pan, W. G. Yang, B. Zou, J. Tang, Z. W. Quan, *Angew. Chem. Int. Ed.* **2017**, *56*, 15969–15973; *Angew. Chem.* **2017**, *129*, 16185–16189.
- [19] G. King, P. M. Woodward, *J. Mater. Chem.* **2010**, *20*, 5785.

- [20] P. Woodward, R. D. Hoffmann, A. W. Sleight, *J. Mater. Res.* **1994**, *9*, 2118.
- [21] V. P. Sakhnenko, N. V. Ter-Oganessian, *Acta Crystallogr. Sect. B* **2018**, *74*, 264.
- [22] S. Vasala, M. Karppinen, *Prog. Solid State Chem.* **2015**, *43*, 1.
- [23] F. Millange, V. Caignaert, B. Domengès, B. Raveau, E. Suard, *Chem. Mater.* **1998**, *10*, 1974.
- [24] T. Shimada, J. Nakamura, T. Motohashi, H. Yamauchi, M. Karppinen, *Chem. Mater.* **2003**, *15*, 4494.
- [25] M. Maryško, V. V. Laguta, I. P. Raevski, R. O. Kuzian, N. M. Olekhovich, A. V. Pushkarev, Y. V. Radyush, S. I. Raevskaya, V. V. Titov, S. P. Kubrin, *AIP Adv.* **2017**, *7*, 056409.
- [26] I. P. Raevski, A. V. Pushkarev, S. I. Raevskaya, N. M. Olekhovich, Y. V. Radyush, S. P. Kubrin, H. Chen, C. C. Chou, D. A. Sarychev, V. V. Titov, M. A. Malitskaya, *Ferroelectrics* **2016**, *501*, 154.
- [27] M. Retuerto, M. J. Martínez-Lope, M. García-Hernández, J. A. Alonso, *Mater. Res. Bull.* **2009**, *44*, 1261.
- [28] Z. Deng, M. Retuerto, S. Liu, M. Croft, P. W. Stephens, S. Calder, W. Li, B. Chen, C. Jin, Z. Hu, M.-R. Li, H.-J. Lin, T.-S. Chan, C.-T. Chen, S. W. Kim, M. Greenblatt, *Chem. Mater.* **2018**, *30*, 7047.
- [29] K. L. Holman, Q. Huang, T. Klimczuk, K. Trzebiatowski, J. W. G. Bos, E. Morosan, J. W. Lynn, R. J. Cava, *J. Solid State Chem.* **2007**, *180*, 75.
- [30] J. Song, B. Zhao, L. Yin, Y. Qin, J. Zhou, D. Wang, W. Song, Y. Sun, *Dalton Trans.* **2017**, *46*, 11691.
- [31] B. H. Toby, *J. Appl. Crystallogr.* **2001**, *34*, 210.
- [32] C. Meneghini, S. Ray, F. Liscio, F. Bardelli, S. Mobilio, D. D. Sarma, *Phys. Rev. Lett.* **2009**, *103*, 046403.
- [33] J.-W. G. Bos, J. P. Attfield, *Chem. Mater.* **2004**, *16*, 1822.
- [34] J. Philipp, P. Majewski, L. Alff, A. Erb, R. Gross, T. Graf, M. Brandt, J. Simon, T. Walther, W. Mader, D. Topwal, D. Sarma, *Phys. Rev. B* **2003**, *68*, 144431.
- [35] D. Choudhury, P. Mandal, R. Mathieu, A. Hazarika, S. Rajan, A. Sundaresan, U. V. Waghmare, R. Knut, O. Karis, P. Nordblad, D. D. Sarma, *Phys. Rev. Lett.* **2012**, *108*, 127201.
- [36] N. V. Ter-Oganessian, V. P. Sakhnenko, **2019**, arXiv: 1902.09579.
- [37] P. Blaha, K. Schwarz, G. K. H. Madsen, D. Kvasnicka, J. Luitz, Technische Universität Wien **2001**, Wien, Austria.
- [38] J. P. Perdew, K. Burke, M. Ernzerhof, *Phys. Rev. Lett.* **1996**, *77*, 3865.
- [39] V. V. Anisimov, I. I. Solovyev, M. A. Korotin, M. T. Czyzyk, G. A. Sawatzky, *Phys. Rev. B* **1993**, *48*, 16929.
- [40] V. I. Anisimov, F. Aryasetiawan, A. I. Lichtenstein, *J. Phys. Condens. Matter* **1997**, *9*, 767.

Manuscript received: February 6, 2020

Accepted manuscript online: March 17, 2020

Version of record online: April 6, 2020